J|A|C|S
A R T I C L E S

Kinetics of the Oxygenation of Unsaturated Organics with Singlet Oxygen Generated from H_2O_2 by a Heterogeneous Molybdenum Catalyst

Bert F. Sels,* Dirk E. De Vos, and Pierre A. Jacobs

Contribution from the Centre for Surface Chemistry and Catalysis, Katholieke Universiteit Leuven, Kasteelpark Arenberg 23, 3001 Heverlee, Belgium

Received August 11, 2006; E-mail: bert.sels@agr.kuleuven.ac.be

Abstract: A heterogeneous catalyst containing MoO_4^{2-} exchanged on layered double hydroxides (Mo-LDHs) is used to produce $^1O_2$ from H_2O_2, and with this dark $^1O_2$, unsaturated hydrocarbons are oxidized in allylic peroxides. The oxidation kinetics are studied in detail and are compared with the kinetics of oxidation by $^1O_2$, formed from H_2O_2 by a homogeneous catalyst. A model is proposed for the heterogeneously catalyzed $^1O_2$ generation and peroxide formation. The model divides the reaction suspension in two compartments: (1) the intralamellar and intragranular zones of the LDH catalyst; (2) the bulk solution. The 2-compartment model correctly predicts the oxidant efficiency and peroxide yield for a series of olefin peroxidation reactions. $^1O_2$ is generated at a high rate by the heterogeneous catalyst, but somewhat more $^1O_2$ is lost by quenching with the heterogeneous catalyst than using the homogeneous catalyst. Quenching occurs mainly as a result of collision with the LDH hydroxyl surface, as is evidenced by using LDH supports containing strong $^1O_2$ deactivators such as Ni^{2+}. A total of 15 organic substrates were peroxidized on a preparative scale using the best Mo-LDH catalyst under optimal conditions.

Introduction

Singlet molecular oxygen is a highly selective and reactive oxidant which is increasingly used in the synthesis of fine chemicals, particularly in the industrial preparation of perfumes and medicinal compounds.[1-4] For instance, $^1O_2$ is employed in the chemical synthesis of artemisisin, the newest type of antimalarial drug.[5] Most procedures for $^1O_2$ generation rely on photochemistry, in which light energy is transferred to molecular dioxygen with the aid of suitable organic sensitizers.[6-8] Despite the success of photochemical procedures at laboratory scale, they have inherent shortcomings for large-scale production.[9] The application of "dark" reactions for the production of $^1O_2$ has therefore attracted increasing interest. The principal reaction is the heterolytic disproportionation of two molecules of H_2O_2 into $^1O_2$ and water. Molybdate, calcium, and lanthanide salts have been reported to catalyze this decomposition very efficiently.[10-12]

Recently we focused on the design of heterogeneous versions of these dark $^1O_2$ generators. The development of cheap, recyclable, and on-to-go catalysts will greatly extend the $^1O_2$ chemistry from today's laboratory scale application to multigram scale processes. While previous immobilization attempts mainly

(1) (a) Frimer, A. A. In *Singlet O_2*; CRC Press: Boca Raton, FL, 1985. (b) Clennan, E. L. *Tetrahedron* **2000**, *56*, 9151. (c) Gollnick K.; Kuhn, H. J. Ene-Reactions with Singlet Oxygen. In *Organic Chemistry, Singlet Oxygen*; Wasserman, H. H., Murray R. W., Eds.; Academic Press: London, 1979; Vol. 40, p 287.

(2) (a) Zhang, D.; Wu, L.-Z.; Yang, Q.-Z.; Li, X.-H.; Zhang, L.-P.; Tung, C.-H. *Org. Lett*. **2003**, *5*, 3221. (b) Ohta, B. K.; Foote, C. S. *J. Am. Chem. Soc*. **2002**, *124*, 12064.

(3) Helesbeux, J. J.; Duval, O.; Guilet, D.; Seraphin, D.; Rondeau, D.; Richomme, P. *Tetrahedron* **2003**, *59*, 5091.

(4) (a) Adam, W.; Bottke, N.; Engels, B.; Krebs, O. *J. Am. Chem. Soc*. **2001**, *123*, 5542. (b) Adam, W.; Bottke, N.; Krebs, O.; Lykakis, I.; Orfanopoulos, M.; Stratakis, M. *J. Am. Chem. Soc*. **2002**, *124*, 14403.

(5) (a) Zhou, W.-S.; Xu, X.-X. *Acc. Chem. Res*. **1994**, *27*, 211. (b) Haynes, K.; Vonwiller, S. C. *Acc. Chem. Res*. **1997**, *30*, 73. (c) O'Neill, P. M.; Posner, G. H. *J. Med. Chem*. **2004**, *47*, 2945. (d) Robert, A.; Dechy-Cabaret, O.; Cazalles, J. M.; Meunier, B. *Acc. Chem. Res*. **2002**, *35*, 167.

(6) (a) Gilbert, A.; Baggott, J. In *Essentials of Molecular Photochemistry*; CRC Press, Blackwell: Boca Raton, FL, 1991; Chapter 11, p 501. (b) Buell, S. L.; Demas, J. N. *J. Phys. Chem*. **1983**, *87*, 4675. (c) Krasnovsky, A. A.; Foote, C. S. *J. Am. Chem. Soc*. **1993**, *115*, 6013. (d) Nau, W. M.; Adam, W.; Scaiano, J. C. *J. Am. Chem. Soc*. **1996**, *118*, 2742.

(7) (a) Gao, R.; Ho, D. G.; Hernández, B.; Selke, M.; Murphy, D.; Djurovich, P. I.; Thompson, M. E. *J. Am. Chem. Soc*. **2002**, *124*, 14828. (b) Jensen, A. W.; Daniels, C. *J. Org. Chem*. **2003**, *68*, 207. (c) Singleton, D. A.; Hang, C.; Szymanski, M. J.; Meyer, M. P.; Leach, A. G.; Kuwata, K. T.; Chen, J. S.; Greer, A.; Foote, C. S.; Houk, K. N. *J. Am. Chem. Soc*. **2003**, *125*, 1319. (d) Jackson, J. A.; Newsham, M. D.; Worsham, C.; Nocera, D. G. *Chem. Mater*. **1996**, *8*, 558.

(8) (a) Li, X.; Ramamurthy, V. *J. Am. Chem. Soc*. **1996**, *118*, 10666. (b) Stratakis, M.; Rabalakos, C.; Mpourmpakis, G.; Froudakis, G. E. *J. Org. Chem*. **2003**, *68*, 2839. (c) Stratakis, M.; Froudakis, G. *Org. Lett*. **2000**, *2*, 1369. (d) Kaanumalle, L. S.; Shailaja, J.; Robbins, R. J.; Ramamurthy, V. *J. Photochem. Photobiol*. **2002**, *153*, 55. (e) Ramamurthy, V.; Shailaja, J.; Kaanumalle, L. S.; Sunoj, R. B.; Chandrasekhar, J. *Chem. Commun*. **2003**, *16*, 1987. (f) Pace, A.; Clennan, E. L. *J. Am. Chem. Soc*. **2002**, *124*, 11236.

(9) Wootton, R. C. R.; Fortt, R.; de Mello, A. J. *Org. Process Res. Dev*. **2002**, *6*, 187.

(10) (a) Dedman, A. J.; Lewis, T. J.; Richards, D. H. *J. Chem. Soc*. **1963**, 2456. (b) Hayashi, V. L.; Shioi, S.; Togami, M.; Sakan, T. *Chem. Lett*. **1973**, 651. (c) Aubry, J. M. *J. Am. Chem. Soc*. **1985**, *107*, 5844. (d) Aubry, J. M.; Cazin, B. *Inorg. Chem*. **1988**, *27*, 2013. (e) Niu, Q. J.; Foote, C. S. *Inorg. Chem*. **1992**, *31*, 3472. (f) Böhme, K.; Brauer, H.-D. *Inorg. Chem*. **1992**, *31*, 3468. (g) Nardello, V.; Marko, J.; Vermeersch, G.; Aubry, J. M. *Inorg. Chem*. **1995**, *34*, 4950. (h) Aubry, J. M.; Bouttemey, S. *J. Am. Chem. Soc*. **1997**, *119*, 5286. (i) Nardello, V.; Bogaert, S.; Alsters, P. L.; Aubry, J. M. *Tetrahedron Lett*. **2002**, *43*, 8731. (j) Nardello, V.; Herve, M.; Alsters, P. L.; Aubry, J. M. *Adv. Synth. Catal*. **2002**, *344*, 184.

(11) (a) Pierlot, C.; Nardello, V.; Schrive, J.; Mabille, C.; Barbillat, J.; Sombret, B.; Aubry, J. M. *J. Org. Chem*. **2002**, *67*, 2418. (b) Trokiner, A.; Bessiere, A.; Thouvenot, R.; Hau, D.; Marko, J.; Nardello, V.; Pierlot, C.; Aubry, J. M. *Solid State Nucl. Magn. Res*. **2004**, *25*, 209.

(12) Nardello, V.; Barbillat, J.; Marko, J.; Witte, P. T.; Alsters, P. L.; Aubry, J. M. *Chem.—Eur. J*. **2003**, *9*, 435.

focused on polystyrene resins[13] and zeolite solid supports,[8] we succeeded in creating a stable inorganic solid catalyst, viz., molybdate exchanged on layered double hydroxides (Mo-LDH).[14] LDHs are hydroxide-type materials with a lamellar structure and an exceptionally high anion exchange capacity.[15] This catalyst is free of metal leaching, easy to handle, and can be prepared in large quantities with standard laboratory equipment.

While the kinetics of peroxide formation are fairly well understood in homogeneous systems, there is a lack of in-depth knowledge on the behavior of $^1O_2$ in solid−liquid mixtures.[16] Data on the lifetime of $^1O_2$ in such heterogeneous mixtures have been reported only sporadically and mainly in the context of oxygen diffusion and adsorption experiments. Despite the importance of $^1O_2$ in organic oxidation, the kinetic information has only scarcely been translated and discussed with regard to reaction productivity. There is general agreement that porous materials, e.g., zeolites and silicas, tend to shorten the lifetime of $^1O_2$.[8f]

We here report on the production of $^1O_2$ from H_2O_2 by MoO_4^{2-}-exchanged layered double hydroxides (Mo-LDHs) and on the usefulness of the $^1O_2$ produced by this system in organic transformations. On the basis of the catalytic results for olefin peroxidation, a general kinetic model is proposed that adequately describes the yields for olefin peroxidation in the heterogeneous catalytic system. A key assumption in the model is the compartmentalization of the reaction suspension in terms of a compartment close to the catalyst, i.e., the intralamellar and intragranular zones, and a second compartment formed by the bulk solution. On the basis of the given amounts of reagents, the model predicts the feasibility of olefin peroxidation in terms of oxidant efficiency and organic peroxide productivity. The model is validated in the preparative peroxidation of 15 substrates, using the best Mo-LDH catalyst in optimal conditions.

Experimental Section

Materials. All materials were used as received. 2,3-Dimethyl-2-butene (DMB), 2-heptanol, and methanol were from Acros, Acros, and Merck, respectively. H_2O_2 was used as a 35% aqueous solution. Magnesium and aluminum salts were purchased from commercial sources in the highest grade and were used as such.

Instrumentation for Analysis. The reaction product 2,3-dimethyl-3-hydroperoxo-1-butene (DMBO$_2$) was analyzed by gas chromatography using a HP 5890 gas chromatograph fitted with a FI detector and a Chrompack CP-Sil 5 column (WCOT, 40 m). Quantification of

DMBO$_2$ was based on the external standard technique using 2-heptanol. Note that, owing to its pronounced stability, this hydroperoxide can easily be analyzed by GC without thermal reduction into the corresponding 2,3-dimethyl-1-buten-3-ol. A precolumn was not used to avoid any peroxide decomposition. Upon contact of the reaction mixture with a reducing agent such as Me$_3$P, the alcohol is formed, which confirms the presence of the hydroperoxide.

General Procedure for Dioxygenation of DMB. A 0.4 mmol amount of DMB (0.1 M) and Mo-LDH are mixed in 4 mL of MeOH and stirred in closed glass bottles. The MoO_4^{2-} concentrations used are specified in the captions of the figures and explained in Table SI1 (Supporting Information). The bottles are placed in a thermostatic bath to keep the reaction temperature constant at 23 ± 0.5 °C throughout the whole experiment. The reaction is initiated after approximately 15 min stirring by addition of 110 μL of 35% H_2O_2 (0.28 M). With regular intervals, minimal samples are withdrawn and quickly centrifuged prior to GC analysis.

Typical Procedure for Preparative Oxygenation. To a stirred suspension of Mo-LDH-**4** catalyst and the substrate (compounds **1**−**15** in Table 2) in 20 mL of solvent, 300 μL of 35 wt % H_2O_2 (or 55 μL for compound **1**) is added. The mixture is stirred at 500 rpm at 30 °C. As soon as the red-brown suspension fades into yellow, a new portion of the oxidant is added. Substrate concentrations, oxidant concentrations, and reaction times are mentioned in Table 2. Product analysis was done with GLC (30 m Chrompack CP-Sil 5 column) after reduction or without reduction. Suitable reducing agents are Na$_2$SO$_3$ and (CH$_3$)$_3$P. GC analyses of the reaction mixtures were compared with those of authentic samples prepared photochemically or in dark conditions, e.g., via the Kasha−Khan reaction. The identity of the organic peroxides was confirmed by 300 MHz ^{1}H and ^{13}C NMR.

Evolution of H_2O_2 Conversion. The evolution of H_2O_2 was followed by cerimetry. A 150 μL sample of the reaction mixture was quickly diluted into 17 mL of water, acidified with H_2SO_4 (7% of the total volume). The titration was performed with Ce(SO$_4$)$_2$·4H$_2$O (0.1 M) using an automatic 725Dosimat (Metrohm).

Determination of $^1O_2$ Yield and Values of β_{APP} (Wilkinson Plot). A 4 mL volume of MeOH was used to dissolve various amounts of DMB: e.g., for homogeneous catalysis, 65.3, 48.3, 34.2, 23.2, 13.4, 10.2, and 4.6 mg or 189, 140, 99, 67, 39, 30, and 14 mM; e.g., for heterogeneous catalysis, 91.9, 61.4, 39.5, 38.5, 13.1, 12.0, 7.6, 6.9, and 5.2 mg or 265.8, 177.5, 114.2, 111.1, 37.9, 34.8, 22.0, 19.9, and 15.1 mM. The heterogeneous reactions were carried out with 0.055 g of Mo-LDH-**2** (or 2.5 mM Mo) in 4 mL of pure MeOH, whereas the homogeneous reactions were performed with 2.5 mM Na$_2$MoO$_4$·2H$_2$O in 0.01 M NaOH in a H_2O/MeOH mixture (15/85 vol %). The reaction was started by adding 110 μL of 35% H_2O_2 (0.28 M) and was stirred magnetically at 25 °C. Each solution was sampled after exactly 68 min and quickly centrifuged (~1 min) in the case of heterogeneous catalysis. To 100 μL of this solution (or supernatant) was added 50 μL of a 2.0 × 10^{-3} M standard solution of 2-heptanol in MeOH. The yields of DMBO$_2$ were determined by GC analysis. For both the homogeneous and heterogeneous set of reactions, an extra reaction was carried out in absence of DMB. After the same reaction time, the amount of H_2O_2 consumed was determined from the latter reactions by following the procedure described earlier. As will be explained, a "Wilkinson plot" can be constructed based on such a data set. Similar sets of data were also gathered for the DMB hydroperoxidation with other Mo-LDH catalysts (Mo-LDH-**1**, -**2**, -**4**, and -**7**) having different Mo loadings and for other substrates (see Table 1).

Synthesis and Characterization of the Mo-LDHs. The preparation of small LDH crystallites is based on the precipitation of the nitrate salts under alkaline conditions at pH = 10 for the Mg$_{0.7}$Al$_{0.3}$(OH)$_2$-{NO$_3^-$}$_{0.3}$·mH$_2$O sample and at pH = 8.5 for the Mg$_{0.7-x}$Ni$_x$Al$_{0.3}$(OH)$_2$-{NO$_3^-$}$_{0.3}$·mH$_2$O samples in slight supersaturation. A detailed procedure can be found elsewhere.[14,17] In a typical anion exchange procedure, the hydrated LDH powder (1 g) is contacted with a solution of Na$_2$-

(13) (a) Blossey, E. C.; Neckers, D. C.; Thayer, A. L.; Schaap, A. P. *J. Am. Chem. Soc.* **1973**, *95*, 5820. (b) Schaap, A. P.; Thayer, A. L.; Blossey, E. C.; Neckers, D. C. *J. Am. Chem. Soc.* **1975**, *97*, 3741. (c) Neckers, D. C.; Blossey, E. C.; Schaap, A. P. Photosensitized reactions utilizing polymer bound photosensitizing catalysts. U.S. Patent 4 315 998, Feb 1982. (d) McGoran, E. C.; Wyborney, M. *Tetrahedron Lett.* **1989**, *30*, 783.

(14) (a) van Laar, F.; De Vos, D.; Vanoppen, D.; Sels, B. F.; Jacobs, P. A.; Del Guerzo, A.; Pierard, F.; Kirsch-De Mesmaeker, A. *Chem. Commun.* **1998**, 267. (b) Sels, B. F.; De Vos, D.; Pierard, F.; Kirsch-De Mesmaeker, A.; Jacobs, P. A. *J. Phys. Chem. B* **1999**, *103*, 11114. (c) De Vos, D.; Wahlen, J.; Sels, B. F.; Jacobs, P. A. *Synlett* **2002**, *3*, 367. (d) De Vos, D.; Sels, B. F.; Jacobs, P. A. *CATTECH* **2002**, *6*, 14. (e) Wahlen, J.; De Vos, D. E.; Sels, B. F.; Nardello, V.; Aubry, J.-M.; Alsters, P. L.; Jacobs, P. A. *Appl. Catal, A: Gen.* **2005**, *293*, 120.

(15) (a) Sels, B. F.; De Vos, D.; Jacobs, P. A. *Catal. Rev.* **2001**, *43*, 443. (b) Trifirò, F; Vaccari, A. Hydrotalcite-like Anionic Clays (Layered Double Hydroxides). In *Comprehensive Supramolecular Chemistry*; Alberti, G., Bein, T., Eds.; Pergamon, Elsevier Science: Oxford, U.K., 1996; Vol. 7, p 251. (c) Rives, V.; Ulibarri, M. A. *Coord. Chem. Rev.* **1999**, *181*, 61.

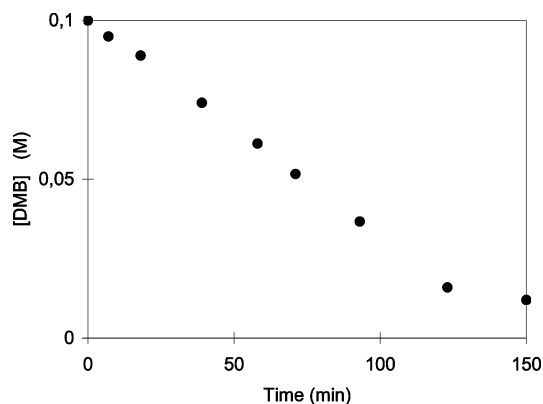(16) Wilkinson, F.; Helman, W. P.; Ross, A. B. *J. Phys. Chem. Ref. Data* **1995**, *24*, 663.

Figure 1. Kinetic profile of the hydroperoxidation of 0.1 M DMB by Mo-LDH-**3** (or 3.6 mM MoO_4^{2-}) plus H_2O_2 (0.28 M) in MeOH at 296 K.

MoO$_4$ (100 mL) overnight under vigorous stirring. The suspension is then subjected to several centrifugation–washing cycles until salt free. The wet cakes were lyophilized to dryness. Analysis for Mo in the centrifugate and in the collected washing waters showed in all cases a more than 95% uptake of the MoO_4^{2-}. This illustrates the known high affinity of the LDH ion-exchanger for MoO_4^{2-}. The techniques used for the characterization of Mo-LDH have been published before.[18]

Semiquantitative ESR Study of Reaction Suspensions. Aliquots of the suspension are taken after 5 min from a typical reaction of hydrogen peroxide (110 μL, 35 wt % in H_2O) with 0.05 g of Mo-LDH in 2 mL of methanol. The samples are immediately frozen with liquid N_2 in ESR tubes. ESR measurements were carried out at 130 K using a Bruker ESP 300 E spectrometer (1 G modulation amplitude; 7–10 dB; 9.5 GHz).

Results

Characterization of Catalysts. Table SI1 (Supporting Information) summarizes the composition of the catalysts synthesized, along with their lattice parameters, sorption characteristics, and acid–base properties. The catalysts have been extensively characterized by IR, Raman, ICP, XRD, SEM, and BET in previous papers.[18] In general, electron micrograph pictures show that the Mo-LDH catalyst can be considered as small plateletlike crystallites agglomerated into large porous granules. The pores are typically in the mesoporous range. The volume of these pores depends on various parameters such as the M^{II}/Al ratio in the Mo-LDH catalyst; in the series of catalysts discussed here, the pore volume, e.g., decreases as the amount of exchanged MoO_4^{2-} increases (Table SI1). The crystallinity of the catalysts was confirmed by X-ray diffraction analysis. The pattern of the reflections in the diffractogram and the lattice parameters deduced from it are characteristic for LDH-like phases. The speciation of the Mo has been studied with a combination of FT-IR and Raman spectroscopy. Irrespective of the Mo surface concentration, the exchanged Mo mainly occurs in the monomeric MoO_4^{2-} form. Characteristic absorption bands are observed near 820–850 cm^{-1} in IR, which can be ascribed to the antisymmetric Mo–O stretching vibration, and at 898, 842, and 317 cm^{-1} in the Raman spectra; the latter are due to the symmetric and antisymmetric Mo–O stretching and the O–Mo–O deformation vibrations, respectively.

Determination of the $^1O_2$ Formation Rate. Since DMB (2,3-dimethyl-2-butene) reacts rapidly with $^1O_2$ yielding DM-

(17) Sels, B. F.; De Vos, D.; Jacobs, P. A. *J. Am. Chem. Soc.* **2001**, *123*, 8350.
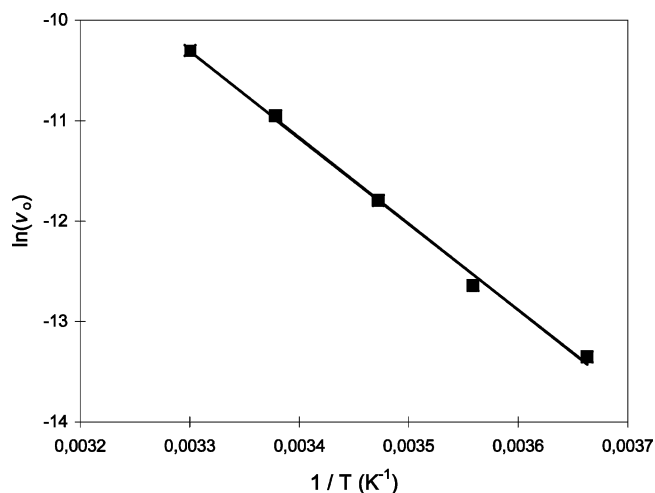(18) Sels, B. F.; De Vos, D.; Grobet, P.; Jacobs, P. A. *Chem.—Eur. J.* **2001**, *7*, 2547.

Figure 2. Arrhenius plot for the hydroperoxidation of 0.1 M DMB in the presence of Mo-LDH-**3**: (■) experimental data points corresponding to results of Figure SI1 (Supporting Information).

BO$_2$, according the *ene* reaction (eq 1), loss of $^1O_2$ due to physical quenching with solvent or substrate molecules can be neglected at sufficient DMB concentrations. Thus, the rate of DMB oxidation, ν_o, equals the rate of $^1O_2$ formation, ν_s. More detailed information concerning the kinetics of $^1O_2$ trapping in homogeneous systems can be found in the Supporting Information. Since both DMB and DMBO$_2$ are easily analyzed by GC, chemical trapping experiments with DMB provide a convenient tool to study the production of $^1O_2$ from homogeneous catalysts.

$$\text{DMB} \xrightarrow{^1O_2} \text{DMBO}_2 \qquad (1)$$
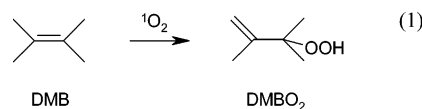
When 0.28 M H_2O_2 is added to a suspension of Mo-LDH-**3** in MeOH containing 0.1 M DMB, the concentration of DMB typically falls as shown in Figure 1. For all sampling points, the hydroperoxide DMBO$_2$ is the principal product, with a selectivity exceeding 94% in all cases. No significant consumption of DMB is observed when H_2O_2 or MoO_4^{2-} is omitted from the reaction suspension.

Figure 1 shows that the peroxidation rate is constant until at least 80% of the substrate consumption, and this rate can be calculated from the slope of the plot. The order of the oxidation with respect to the trapping agent DMB is thus zero, implying that, at least in the initial phase of the reaction, the DMB concentration is sufficiently high to trap any $^1O_2$ that is available in the solution. Thus, when 0.28 M H_2O_2 is added to 2.5 mM MoO_4^{2-} on LDH in MeOH at 296 K, $11.8 \pm 0.7 \times 10^{-6}$ M $^1O_2$/s is released into the reaction solution and is trapped by DMB.

Influence of the Temperature. Using the procedure described earlier, values of the oxidation rate ν_o were calculated from experiments in which the temperature was varied between 0 and 30 °C. Initial H_2O_2, DMB, and MoO_4^{2-} concentrations were kept constant at 0.28 M, 0.1 M, and 3.6 mM, respectively. The time profiles for the reactions are given in the Supporting Information (Figure SI1). For all reaction temperatures, hydroperoxide selectivity was over 94% at total H_2O_2 conversion. Again, DMB linearly disappears with time. Figure 2 shows the
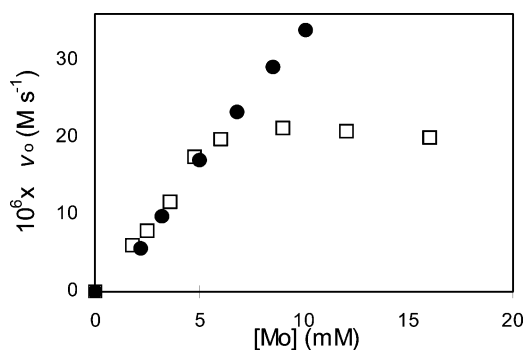
Figure 3. Influence of the Mo concentration on the hydroperoxidation rate (0.1 M DMB): (●) with variation of the total weight of added catalyst using catalyst Mo-LDH-**3**; (□) by variation of the degree of MoO_4^{2-} exchange of the LDH support.

corresponding Arrhenius plot. From the slope, the apparent activation energy is calculated, yielding $E_a = 66.5 \pm 7.5$ kJ·mol^{-1}.

Influence of Variable [Mo]$_T$. Experiments in which the total concentration of Mo ([Mo]$_T$) was varied in the range of 1.5–16 mM were conducted in two ways: (a) The oxygenation was studied by changing the amount of catalyst with fixed MoO_4^{2-} loading—in this experiment a Mo-LDH-**3** was used. (b) The oxygenation was studied using Mo-LDHs with varying MoO_4^{2-} loading (Mo-LDH-**1** to -**8**). The concentrations of H_2O_2 and DMB were kept constant at 0.28 and 0.1 M, respectively, and the reactions were performed in MeOH at 296 K. The dependence of v_o on [Mo]$_T$ for experiments a and b is summarized in Figure 3.

The results of experiment a show that v_o increases almost linearly when increasing the amount of Mo-LDH, indicating a first-order dependence on MoO_4^{2-}. The slope gives the oxidation rate (M·s^{-1}) per mole of MoO_4^{2-} and equals $3.6 \pm 0.4 \ 10^{-3}$ s^{-1} for the conditions used (i.e., in MeOH, 296 K, and [H_2O_2] = 0.28 M).

By variation of [Mo]$_T$ by method b, a similar linearity was observed with respect to [Mo]$_T$ for concentrations in the range of 1.8–4.8 mM, i.e., for MoO_4^{2-} loadings between 8% and 22% of the total anion exchange capacity (AEC $\sim$ 3.3 mequiv·g^{-1}). The slope ($3.4 \pm 0.2 \ 10^{-3}$ s^{-1}) of the curve agrees within experimental error with that obtained via method a. However, at higher Mo loadings, the linearity is disturbed and v_o becomes independent of [Mo]$_T$. This inflection point corresponds to a critical Mo loading of 20–25% of the total AEC ($\sim$3.3 mequiv·g^{-1}) and a maximum v_o of about 20×10^{-6} M·s^{-1}.

Influence of [H_2O_2]$_0$. To study the influence of the initial hydrogen peroxide concentration [H_2O_2]$_0$, experiments were conducted with 0.1 M DMB at 296 K in MeOH, with a constant [Mo]$_T$ of 1 mM. Both the soluble Na_2MoO_4 and the heterogeneous Mo-LDH-**3** catalysts were investigated. Note that the experiments with Mo-LDH-**3** were conducted in MeOH, whereas the reactions with Na_2MoO_4 were performed in aqueous MeOH (85/15 vol % for MeOH/H_2O), because of the poor solubility of Na_2MoO_4 in neat MeOH. The dependence of v_o on [H_2O_2]$_0$ up to 0.30 M is depicted in Figure 4. As can be seen, the kinetics with regard to H_2O_2 are complex, showing an asymmetric bell shape for both systems. By the increase of [H_2O_2]$_0$, the rate of disappearance of DMB (v_o) initially rises, then reaches a well-defined maximum, and finally gently decreases. Note that the peroxidation rates are significantly
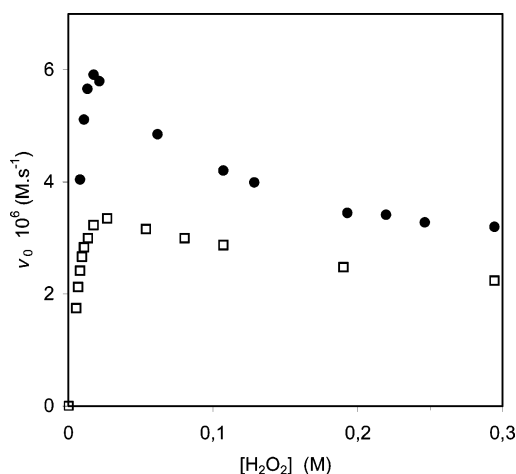

Figure 4. Influence of the initial [H_2O_2]$_0$ on the hydroperoxide formation rate v_o in the presence of (●) Mo-LDH-**2** and (□) Na_2MoO_4 (0.1 M DMB, [Mo]$_T$ = 1 mM).

higher for the Mo-LDH/H_2O_2 system than for the soluble catalyst. For the homogeneous system, the maximum value for v_o equals $(3.4 \pm 0.2) \times 10^{-6}$ M s^{-1} at [H_2O_2]$_0$ = 0.030 M, whereas for the heterogeneous system v_o is $(5.9 \pm 0.3) \times 10^{-6}$ M s^{-1} at [H_2O_2]$_0$ = 0.020 M.

Influence of the Substrate Concentration. To examine the effect of the initial DMB concentration [DMB]$_0$ on v_o, a series of experiments was carried out with [H_2O_2]$_0$ = 0.28 M and [Mo]$_T$ = 2.5 mM at 296 K, with homogeneous and heterogeneous catalysts. In this series, the concentration of DMB was varied from 0.01 to 0.3 M. All reactions were analyzed after exactly 68 min. Figure 5 displays the plot of the yield of DMBO$_2$ versus [DMB]$_0$. The curves of Figure 5 display a clear plateau, which is characteristic for trapping of ${}^1O_2$ using reactive acceptors. Indeed, when sufficient DMB is available, all ${}^1O_2$ produced is consumed in the chemical reaction.

Even more important is the quantitative information that can be extracted when the data of Figure 5 are plotted in a way analogous to equation SI8 (Supporting information). Dividing equation SI 8 by the total amount of H_2O_2 consumed results in the following expression, in which Y is the yield of the DMB oxidation based on the oxidant used:

$$Y = \frac{[DMB]_0 - [DMB]_t}{[H_2O_2]_0 - [H_2O_2]_t} = \left(\frac{k_r}{k_r + k_q}\right)\left(\frac{[{}^1O_2]_{total}}{[H_2O_2]_0 - [H_2O_2]_t}\right) -$$
$$\left(\frac{k_d}{k_r + k_q}\right)\left\{\frac{\ln\left(\frac{[DMB]_0}{[DMB]_t}\right)}{[H_2O_2]_0 - [H_2O_2]_t}\right\}$$

$$Y = \gamma Y_0 - \beta X \tag{2}$$

Here [${}^1O_2$]$_{total}$ is the cumulative concentration of ${}^1O_2$ after time t, i.e., the ${}^1O_2$ concentration that would be present in the reaction mixture if ${}^1O_2$ were not quenched at all by the substrate DMB or by the solvent and $Y_0 = [{}^1O_2]_{total}/([H_2O_2]_0 - [H_2O_2]_t)$. According to eq 2, $Y = ([DMB]_0 - [DMB]_t)/([H_2O_2]_0 - [H_2O_2]_t)$ can be plotted versus $X = \ln([DMB]_0/[DMB]_t)/([H_2O_2]_0 - [H_2O_2]_t)$. In these so-called Wilkinson plots, a straight line is normally obtained, with γY_0 as intercept with the vertical axis and β as slope. For homogeneous systems, the meaning of the slope and intercept in eq 2 is particularly well understood.
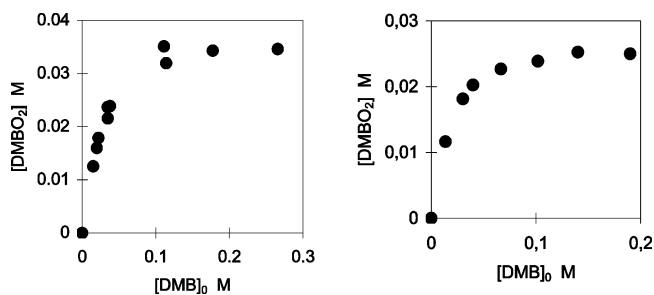
Figure 5. DMBO$_2$ yields as a function of initial alkene concentration for Mo-LDH-**2** (left) and MoO$_4^{2-}$ (right).
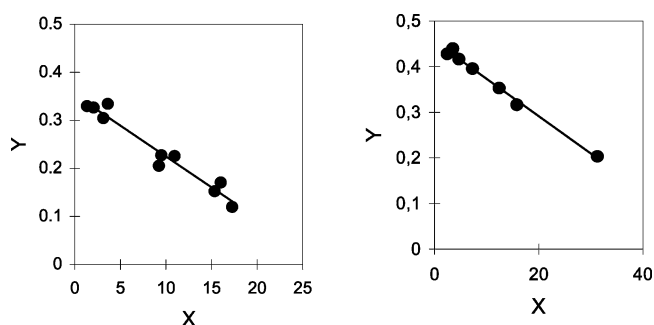

Figure 6. Wilkinson plots for DMB peroxidation in methanolic solvent conditions. The singlet oxygen is produced from 0.28 M H$_2$O$_2$, with the catalysts Mo-LDH-**2** (left) or MoO$_4^{2-}$ (right) at 296 K with [Mo]$_T$ = 2.5 mM. Samples are taken after 68 min and immediately analyzed with GC. H$_2$O$_2$ is titrated with 0.1 N Ce^{4+}. *X* and *Y* are clarified in the text.

The ratio $\gamma = k_r/(k_r + k_q)$ expresses the contribution of the chemical reaction to the overall deactivation by the substrate. Since physical quenching is negligible in the peroxidation of DMB, i.e., $k_q \ll k_r$, γ can be set to unity.[16] The ratio $\beta = k_d/(k_r + k_q)$, known as the "Foote reactivity index", gives the minimum DMB concentration required so that the physical and chemical interaction of ^{1}O$_2$ with DMB dominates over the deactivation by the solvent. Since this value is characteristic for a given trapping agent and a given solvent, it is often used to verify ^{1}O$_2$ involvement. Reference lists with values for β, k_r, and k_q have been reported.[16] Finally, $Y_0 = [^1\text{O}_2]_{\text{total}}/([\text{H}_2\text{O}_2]_0 - [\text{H}_2\text{O}_2]_t)$ equals the ^{1}O$_2$ yield on the basis of the oxidant used, or the overall oxidant efficiency for ^{1}O$_2$ production, defined as the total molar amount of ^{1}O$_2$ available in solution (for interaction with substrate or solvent) per mol of H$_2$O$_2$ consumed. Obviously, as one molecule of ^{1}O$_2$ is formed from two molecules of H$_2$O$_2$, the maximum theoretical value for Y_0 is 0.5.

The kinetic data for DMB peroxidation and H$_2$O$_2$ consumption after 68 min (Figure 5) were converted to a Wilkinson plot, not only for the MoO$_4^{2-}$ reaction but also for the heterogeneously catalyzed LDH-MoO$_4^{2-}$ reaction (Figure 6). From these plots, values can be calculated for the parameters Y_0 and β. For the homogeneous system, a β value of 0.0075 ± 0.002 M was obtained. This value is in good agreement with the calculated β value of DMB for this particular solvent mixture.[16] For Y_0, a value equal to 0.46 ± 0.02 was found. This value compares well with reported values[10] and confirms that practically 1 mol of ^{1}O$_2$ is formed from 2 mol of H$_2$O$_2$.

Parameters were also calculated from the plot for the heterogeneous catalyst Mo-LDH-**2**. Since the physical meaning of these parameters is not necessarily the same as for the homogeneous system, these parameters are denoted as *apparent* β and *apparent* Y_0 values. From Figure 6, β_{app} is 0.011 ± 0.003

Table 1. Wilkinson Plot Data for Mo-LDH Catalysts with Varying MoO$_4^{2-}$ Content and Various Substrates and Conditions as in Figures 5 and 6

substrate	catal	wt (g)	$Y_{0,\text{app}}$	β_{app} (M)	R^2
2,3-dimethyl-2-butene	MoO$_4^{2-}$		0.46	0.0075	0.99
	Mo-LDH-**1**	0.110	0.38	0.011	0.98
	Mo-LDH-**2**	0.055	0.36	0.011	0.97
	Mo-LDH-**4**	0.041	0.31	0.015	0.98
	Mo-LDH-**7**	0.020	0.21	0.025	0.95
2,3-dimethyl-2-butene	Mo-LDH-**2**	0.055	0.36	0.011 (0.0035)^a	0.97
2-methyl-2-butene			0.34	0.15 (0.11)^a	0.95
2-methyl-2-pentene			0.34	0.18 (0.15)^a	0.95
1-methyl-1-cyclohexene			0.29	0.54 (0.53)^a	0.94

^{a} β values in homogeneous solution.[16]

M, while $Y_{0,\text{app}} = 0.38 \pm 0.03$. Since this β_{app} value is significantly higher than that reported for pure MeOH ($\beta_{\text{MeOH}} = 0.004$ M),[16] physical quenching is apparently more pronounced in the solid−liquid system. The lower oxidant efficiency Y_0 for the heterogeneous Mo-LDH system implies that considerably less than 0.5 mol of ^{1}O$_2$ is available in solution/ mol of H$_2$O$_2$ that is disproportionated. This is a clear difference with the common idea on H$_2$O$_2$ decomposition by MoO$_4^{2-}$, namely that ^{1}O$_2$ formation is almost quantitative. This anomaly, along with the lower apparent lifetime of ^{1}O$_2$, will be taken in hand in the Discussion.

The characteristic Wilkinson parameters for the hydroperoxidation of substrates other than DMB are gathered in Table 1. Again, the efficiencies Y_0 for ^{1}O$_2$ production are smaller than 0.5. The same table also summarizes data for Wilkinson plots obtained for DMB in presence of various Mo-LDH catalysts having various concentrations of MoO$_4^{2-}$. Thus, it appears that the least-squares linear fit of eq 2 not only holds for the soluble catalyst and Mo-LDH-**2** but also for the catalysts having higher Mo loadings. The apparent efficiency of the oxidant ($Y_{0,\text{app}}$) decreases with increasing Mo content, whereas the apparent Foote index β_{app} tends to increase with increasing Mo content.

Semiquantitative ESR Spectroscopy. According to Nardello et al.,[10d] the quantitative conversion of H$_2$O$_2$ into ^{1}O$_2$ can only be rationalized on the basis of heterolytic pathways. Indeed, if the decomposition involved homolytic routes, the reactive oxygen radicals would undergo an intersystem crossing with formation of ground-state dioxygen ^{3}O$_2$. Hence, if the decomposition of H$_2$O$_2$ by MoO$_4^{2-}$ or Mo-LDH exclusively occurs via nonradical pathways, the reaction suspension must be ESR silent.

Figure 7 shows, for various Mo-LDH catalysts, the X-band ESR spectra of the frozen suspensions during the initial stage of the H$_2$O$_2$ decomposition. As was demonstrated earlier,[14b] the decomposition of H$_2$O$_2$ by homogeneous MoO$_4^{2-}$ produces only traces of radicals, which is in agreement with the high efficiency of ^{1}O$_2$ generation with soluble MoO$_4^{2-}$. For Mo-LDH-**1**, which has the lowest Mo content, the signal is of a comparable weakness, proving that the selective heterolytic generation of ^{1}O$_2$ from H$_2$O$_2$ is not disturbed by heterogenization of MoO$_4^{2-}$.

However, when the Mo loading of the catalyst is increased, the intensity is remarkably amplified. The shape of the signal is indicative of the axial symmetry of superoxo-type radicals. On the basis of the calculation of the g parameters ($g_\perp = 2.023$, $g_{||} = 2.063$), it can be stated, however, that this species is not a free superoxo radical anion O$_2^{-\circ}$ ($g_\perp = 2.023$ and $g_{||} = 2.092$). A Mo^V−OO$^\circ$ type radical, which might be formed by homolysis

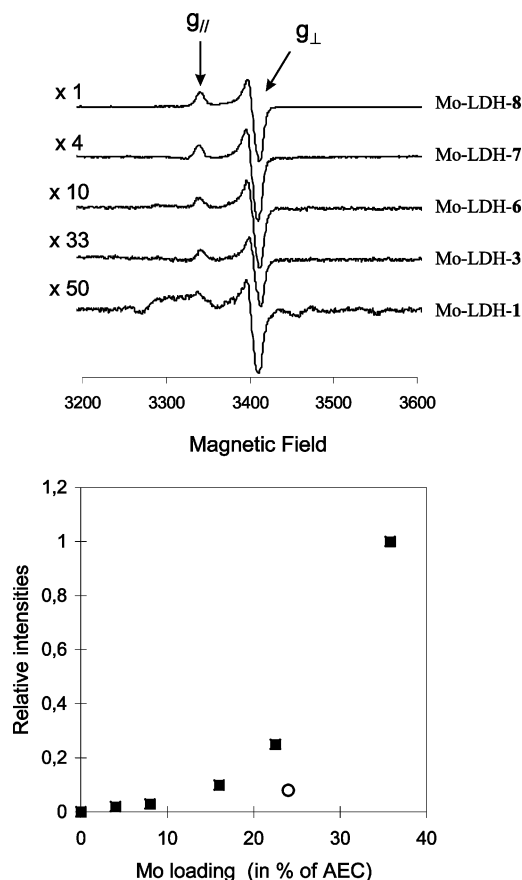**Figure 7.** Top: X-band ESR spectra (130 K) of quickly frozen suspensions of LDH-MoO_4^{2-} in $MeOH/H_2O_2$. Conditions: 0.05 g of LDH catalyst with MoO_4^{2-} content of 66% (Mo-LDH-**8**), 44% (Mo-LDH-**7**), 32% (Mo-LDH-**6**), 16% (Mo-LDH-**3**), and 8% (Mo-LDH-**1**) of total AEC (3.3 mequiv g^{-1}); 2 mL of MeOH; 110 μL of 35% H_2O_2; 300 K, 5 min. Bottom: (■) Relative intensities of ESR signals as obtained by double integration, for suspensions containing 0.05 g of LDH, and (○) ESR signal intensity obtained with 0.15 g of Mo-LDH-**3**.

of a side-on bound peroxo ligand in a peroxomolybdate, can also be discarded, because this reaction would in addition produce a signal of Mo^V. A plausible explanation for the ESR signal is that $O_2^{-\circ}$ is formed and is subsequently stabilized by LDH lattice cations, e.g., as $Mg^{2+}-O_2^{-\circ}$, via ligand exchange of a hydroxyl anion for a superoxo radical anion. Such a process is in line with the upfield shift of the parallel component of the **g** tensor; a similar $g_{\parallel}$ parameter is observed for the superoxo radical bound to, e.g., Ba^{2+}.[19]

Double integration of the ESR signals gives an idea of the relative radical concentrations in the suspensions (Figure 7, lower part). It appears that the intensity of the radical signal increases spectacularly with the MoO_4^{2-} loading. In contrast, tripling the amount of Mo-LDH-**3** increases the signal intensity only by a factor of about 3. Thus, the signal obtained for the frozen H_2O_2-exposed Mo-LDH-**3** (0.15 g solid) suspension is much weaker than that for the suspension with Mo-LDH-**8** (0.05 g of solid but with a 4-fold higher Mo loading). Therefore, it is tentatively proposed that the radical decomposition route involves at least two Mo ions, in contrast to the unimolecular decomposition in the $^1O_2$ formation. At this moment, however,

(19) Rabo, J. A. *Salt Occlusion in Zeolites* in *Zeolite Chemistry and Catalysis*; Rabo, J. A., Ed.; American Chemical Society: Washington, DC, 1976; Vol. 5, p 332.

the exact mechanism for the radical decomposition is unknown. Anyway, it is clear that a radical decomposition process competes with $^1O_2$ formation in the heterogeneous system, at least if Mo-LDH with high Mo loadings is used.

Preparative Peroxidation. To demonstrate the usefulness of the model, oxygenations of several reactive organic substrates were carried out on a preparative scale. The substrates include polycyclic aromatics **1** and **2**, one conjugated diene **3**, several olefins **4**−**7** and **12**−**14**, allylic alcohols **8**−**11**, and one phenolic compound **15**. Some of them have been used in industry since years in the fine chemicals production.[1] The oxidation reactions cover the two most important reaction modes of $^1O_2$: the ene hydroperoxidation (entries **4**−**14**) and the [2 + 4] cycloaddition (entries **1**−**3**). The results of the preparative experiments are tabulated in Table 2. As can be seen, the oxidation is reasonably fast and leads to useful yields for many substrates. The separation of the Mo-LDH catalyst from the reaction products is easily performed by a simple centrifugation or filtration. A specific problem often encountered in heterogeneous catalysis is leaching of the metal ions into the solution. For the Mo-LDH, leaching was quantified by measuring the amount of Mo present in the liquid phase by means of plasma emission spectroscopy (ICP). Experimental results show that the concentration of Mo in the filtrate is systematically lower than 2 ppm. The degree of leaching is therefore below 0.4%.

Since the heterogeneous system operates with maximal rates in less concentrated peroxide solutions, the total amount of H_2O_2 was added in portions, as described in the Experimental Section. Each portion contains 50 equiv of peroxide with respect to Mo. On the other hand, to keep the oxidant efficiency as high as possible, Mo-LDHs having not too high Mo loadings are preferably used. The experiments in the Table 2 have been carried out with Mo-LDH-**4**.

Discussion

Reliability of the Data Analysis. The straightforward and correct nature of our experimental approach using DMB is confirmed by the close agreement of the results with known data on the kinetic properties of $^1O_2$. Indeed, from the kinetics of the soluble MoO_4^{2-} catalyst (Figure 5), a lifetime value of $\tau = 4.1 \pm 0.6$ μs can be calculated for $^1O_2$ in the $MeOH:H_2O$ mixture. This value $\tau = k_d^{-1}$ is obtained from $\beta = k_d/(k_r + k_q) = 0.0075$ (Table 2), with $k_r = 3.3 \times 10^7$ M^{-1} s^{-1} and $k_q \sim 10^3$ M^{-1} s^{-1}.[16] Within experimental error, this is in agreement with the expected values (e.g., $\tau = 3.5$ μs)[16] for the solvent mixture used. Moreover, the oxidant efficiency $Y_0 = 0.46 \pm 0.02$ implies that the production of $^1O_2$ is more or less quantitative, which is consistent with experimental findings from trapping and NIR spectroscopy.[10] Therefore, it may be stated that trapping with DMB is an experimentally sound method to study $^1O_2$ kinetics.

Kinetic Model for $^1O_2$ Generation in a Suspension. Equations SI1−SI5 (Supporting Information) adequately describe the kinetic behavior of $^1O_2$ in a *homogeneous liquid* system. However, to understand the physical meaning of the data for the *solid−liquid* system, a new kinetic model is needed. The pictorial representation of this model is given in Scheme 1. In the model, the LDHs are considered as porous granules, which consist of aggregated LDH crystals. As LDHs are strongly hydrophilic and charged materials, a hydrophobic organic substrate A would rather reside in the bulk of the liquid than

Table 2. Oxygenation of Organic Compounds by the $^1O_2$-Producing System Mo-LDH-**4**/H_2O_2 at 30 °C

	Substrate (mM)	Product(s) (Product distribution)[a]	H_2O_2 (mM) (time / min)	Mo (mM) (solvent)	Yield (%) (Selectivity)
1	[structure] **1**	[structure]	30 (150)	0.15 (Dioxane)	92 (100)
2	[structure] **35**	[structure]	165 (280)	0.45 (THF)	96 (99)
3	[structure] 500	[structure]	2640 (720)	2.8 (MeOH)	90 (91)
4	[structure] 750	[structure] —OOH	2640 (720)	2.8 (MeOH)	97 (98)
5	[structure] 650	[structure] 45 : 55	4455 (608)	5.6 (MeOH)	81 (98)
6	[structure] 650	[structure] 4 : 44 : 52	4455 (724)	5.6 (MeOH)	84 (97)
7	[structure] 500	[structure]	3795 (520)	5.6 (MeOH)	82 (96)
8	[structure] 600	[structure] 58 : 42	4950 (675)	5.6 (MeOH)	88 (92)
9	[structure] 600	[structure] 46 : 54	4950 (675)	5.6 (MeOH)	88 (92)
10	[structure] 600	[structure] 53 : 47	4950 (675)	5.6 (MeOH)	91 (95)
11	[structure] 600	[structure] 41 : 59	4950 (675)	5.6 (MeOH)	82 (94)
12	[structure] 450	[structure]	2145 (585)	2.8 (MeOH : Dioxane)	55 (57)[b]
13	[structure] 350	[structure]	3960 (540)	5.6 (MeOH : Dioxane)	40 (90)
14	[structure] 350	[structure] 76 : 24	3960 (540)	5.6 (MeOH : Dioxane)	76 (90)
15	[structure] 350	[structure]	4455[c] (540)	5.6 (MeOH : Dioxane)	21 (90)

[a] Based on ^1H NMR, ^{13}C NMR and GC-MS. [b] $^1O_2$ is produced by a solid Mo-LDH catalyst. [c] The value presents the selectivity of the *trans*-pinocarveyl hydroperoxide, as illustrated in the table. The total selectivity for hydroperoxides is larger than 90%. [c] 50% aqueous H_2O_2 is used instead of 35%.

close to the solid. Due to such partitioning, the equilibrium concentration of a substrate A inside a porous LDH granule is lower than in the surrounding liquid. For convenience, it is assumed that the concentration of A ([A]) follows a step profile as shown in Scheme 1. This implies that the liquid system is divided into two compartments: (1) the bulk solution ("out") and (2) an intragranular compartment ("in"), with a much lower

Scheme 1. Schematic Representation of the Solid−Liquid System Used to Peroxidize Organic Substrates with H_2O_2 as the Oxidant
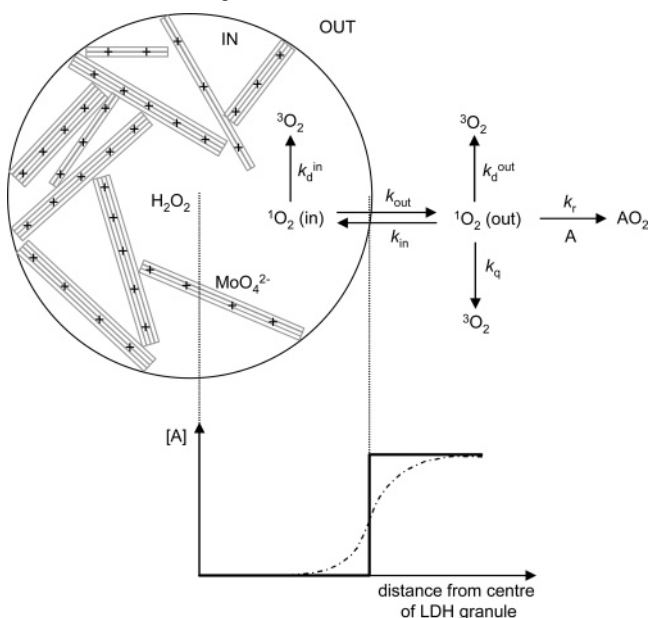

substrate concentration than in the bulk ([A]$_{in}$ $\cong$ 0). $^1O_2$ is chemically generated in the inner compartment from H_2O_2. As soon as $^1O_2$ is formed, it may decay in the inner compartment (k_d^{in}) or it may diffuse into the bulk (k_{out}). In the bulk, $^1O_2$ can either be quenched by the solvent ($k_d^{out} = k_d$ for the solvent composition) or by the substrate (k_q); it can oxygenate the substrate A to form AO_2 (k_r), or it can reenter an LDH granule (k_{in}). Note that because of its hydrophilic nature, H_2O_2 will be abundantly available in the inner compartment.

According to the proposed model, the rate equation for $^1O_2$ in the two different compartments is given by eqs 3 and 4 for the inner and outer compartments, respectively:

$$\frac{d[^1O_2]_{in}}{dt} = \frac{\alpha}{2f}\frac{d[H_2O_2]}{dt} - (k_d^{in} + k_{out})[^1O_2]_{in} + k_{in}[^1O_2]_{out} \quad (3)$$

$$\frac{d[^1O_2]_{out}}{dt} = -\{k_d^{out} + (k_r + k_q)[A]_{out}\}[^1O_2]_{out} + k_{out}\frac{f}{(1-f)}[^1O_2]_{in} - k_{in}\frac{f}{(1-f)}[^1O_2]_{out} \quad (4)$$

The parameter $f = V_{in}/(V_{in} + V_{out})$ takes into account the ratio between the volumes V_{in} and V_{out} of the inner and outer compartments. As will be demonstrated, exact knowledge of f is not required in applying the model. Concentrations with the suffixes "out" or "in" refer to the inner or outer compartments; if no suffix is given, the concentration is given over the whole reaction volume ($V_{in} + V_{out}$). In eq 3, the decomposition rate $d[H_2O_2]/dt$ can be defined as v_{HOOH}; this rate was studied in detail earlier.[18] Possible formation of radicals is accounted for by introducing α, which is defined as the fraction of H_2O_2 that is disproportionated into $^1O_2$. Thus, in a heterogeneous system, equation SI1 (Supporting Information) is better replaced by eq 5:

$$2H_2O_2 \xrightarrow{\text{LDH-MoO}_4^{2-}} \alpha^1O_2 + (1-\alpha)^3O_2 + 2H_2O \quad (5)$$
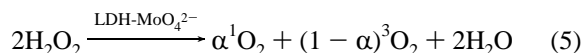
Hence, $v_s = \alpha v_{HOOH}/2$, with v_s the rate of singlet oxygen formation.

Taking into account the simplifying assumption that only $^1O_2$ in the outer compartment is involved in the peroxidation, eqs 3 and 4 can be simplified into eq 6, in which the *escape ratio q* $= k_{out}/(k_d^{in} + k_{out})$ expresses the fraction of $^1O_2$ that actually arrives in the bulk without being quenched inside the LDH granules:

$$\frac{[DMB]_0 - [DMB]_t}{[H_2O_2]_0 - [H_2O_2]_t} = \alpha q \frac{1}{2}\left(\frac{k_r}{k_r + k_q}\right) -$$

$$\left(\frac{k_d^{out}(1-f) + (1-q)k_{in}f}{k_r + k_q}\right)\left\{\frac{\ln\left(\frac{[DMB]_0}{[DMB]_t}\right)}{[H_2O_2]_0 - [H_2O_2]_t}\right\} \quad (6)$$

Using the parameter γ, and with the same X and Y parameters as before, eq 6 can be simplified into eq 7:

$$Y = \frac{1}{2} q\gamma\alpha - \beta_{app}X$$

with

$$\beta_{app} = \left(\frac{k_d^{out}(1-f) + (1-q)k_{in}f}{k_r + k_q}\right)$$

$$q = \frac{k_{out}}{(k_{out} + k_d^{in})} \quad (7)$$

This expression bears a more than superficial similarity to that for the homogeneous reactions (eq 2). Likewise, a plot of Y against X should give a straight line with $1/2\gamma q\alpha$ or $\gamma Y_{0,app}$ as intercept and with β_{app}, instead of β, as the slope. Since the data for the heterogeneously catalyzed peroxidation of DMB show adequate linearity in the $Y-X$ Wilkinson-like plots (Figure 6, left), the model may well be valid, despite the assumptions made.

Interpretation of the Kinetic Data. If one looks at the peroxidation kinetics with $^1O_2$ in heterogeneous conditions (Mo-LDH in methanolic solvents), three observations merit attention.

First, the kinetic data of the peroxidation accord reasonably well with the kinetics of the decomposition of H_2O_2 (see ref 18): The activation energy for the peroxidation of DMB (66.5 $\pm$ 7.5 kJ·mol^{-1}) is close to the 72.7 $\pm$ 6.7 kJ·mol^{-1} obtained earlier for the decomposition of H_2O_2. This close agreement is in line with the fact that peroxidation of organics by $^1O_2$ is generally fast. The rate-determining step in the overall catalytic process is therefore the disproportionation of the peroxomolybdate complexes, with $^1O_2$ formation, rather than the peroxidation. While the peroxidation rate ν_o is proportional with the catalyst concentration $[MoO_4^{2-}]$ at low Mo content of the solid, the order in MoO_4^{2-} becomes zero when the Mo concentration is raised by further increasing the Mo content of the solid (Figure 3). The similar behavior of the decomposition rate ν_{HOOH} was explained in terms of a rate-limiting diffusion of H_2O_2 to the intercalated Mo anions. Moreover, it can be assumed that even if $^1O_2$ is formed by intercalated Mo anions, it will be rapidly deactivated in the confinement of the interlayers. Finally, it was found that, at high Mo loadings, H_2O_2 is not only converted into $^1O_2$. Considerable amounts of radicals are also produced, as proven by ESR (Figure 7). The complex kinetic dependence of the peroxidation rate on the hydrogen peroxide concentration is also analogous to that of the H_2O_2 decomposition rate. That peroxidation rates are higher with MoO_4^{2-} immobilized on the LDH than with dissolved MoO_4^{2-} is ascribed to the labilization of the peroxocomplexes at the LDH surface.

Second, the formation of singlet oxygen and the ensuing peroxidation seem less efficient with respect to H_2O_2 using LDH-MoO_4^{2-} than using dissolved MoO_4^{2-}, i.e. the apparent $^1O_2$ yield $Y_{0,app}$ is smaller for the heterogeneous than for the homogeneous system. According to the model, $Y_{0,app} = (q\alpha)/2$. The lower $^1O_2$ yield in the heterogeneous system can therefore partly be explained by a less efficient production of $^1O_2$ with the immobilized MoO_4^{2-}. Homolytic side reactions decrease the factor α, particularly at high MoO_4^{2-} loadings ($\nu_s = \alpha\nu_{HOOH}/2$). However, since even at low MoO_4^{2-} contents less than 80% of the H_2O_2 is eventually used for peroxidation (Table 1), there must be additional losses of $^1O_2$. A q value smaller than one accounts for these supplementary $^1O_2$ losses. Physically, the q value expresses the probability that a $^1O_2$ molecule reaches the solution containing the target substrate instead of being quenched inside a LDH granule. Hence, the Wilkinson plots for a Mo-LDH with low Mo content show that about 20−30% of the produced $^1O_2$ molecules are deactivated before they are able to peroxidize the substrate ($q = 0.76$ with $\alpha \sim 1$). Quenching of $^1O_2$ is probably promoted by the high anion and surface hydroxyl concentration.[20] A quantitative study of quenching by surface hydroxyls has been performed by Thomas and Iu, using sensitizers adsorbed at mesoporous amorphous silica gel.[20a−c] They discovered that reduction of the $^1O_2$ lifetime is more pronounced in small pores as a consequence of a higher rebound frequency of diffusing $^1O_2$ molecules against the walls. Adsorbed water and silanol surface groups were identified as the effective deactivators. In the proposed model, the decrease of $Y_{0,app}$ is only determined by catalyst-specific effects, as expressed in α and q. This implies that irrespective of the substrate used, the same $Y_{0,app}$ should be obtained for the same catalyst. Wilkinson plots for oxidation of 2,3-dimethyl-2-butene, 2-methyl-2-butene, or 2-methyl-2-pentene using Mo-LDH-**2** result in closely similar $Y_{0,app}$ values, which corroborates the validity of the model. Only for 1-methyl-1-cyclohexene, a lower $Y_{0,app}$ value is found, but this might be due to the poor reactivity of this substrate and, consequently, the larger errors in determining peroxidation yields.

Third, the apparent lifetime of $^1O_2$ is smaller in the heterogeneous conditions, i.e., $\beta_{app} > k_d/(k_r + k_q)$. This means that the heterogeneous reaction medium contains extra deactivation pathways in comparison with the homogeneous solution. Obviously, quenching inside the LDH granules (k_d^{in}) is such a $^1O_2$ deactivation route. The impact of this quenching is more pronounced as more $^1O_2$ fails to escape to the solution, i.e., as the escape ratio q decreases. This is also clarified by rewriting the expression for β_{app}:

$$\beta_{app} = \left(\frac{k_d^{out}}{k_r + k_q}\right)(1-f) + (1-q)f\left(\frac{k_{in}}{k_r + k_q}\right) = \beta(1-f) +$$
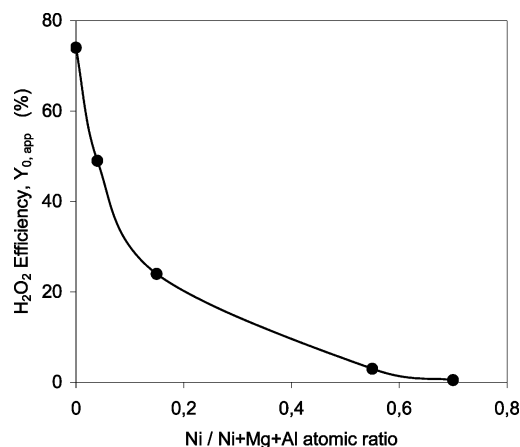
$$(1-q)f\left(\frac{k_{in}}{k_r + k_q}\right) \quad (8)$$

Figure 8. Efficiency of $^1O_2$ trapping by DMB (0.1 M) during the decomposition of H_2O_2 in the presence of various Ni-containing MgAl LDHs exchanged with molybdate. $Y_{0,app}$ is the oxidant efficiency extrapolated for high DMB concentration in the heterogeneous conditions as determined from Wilkinson plots.

Figure 9. Graphical representation of the kinetic model. The Y axis gives the estimated concentration of the oxidant as a function of the required substrate conversion in the peroxidation of substrate A using catalyst Mo-LDH-**2** in MeOH. Symbols used in the X and Y axis are explained in the text.

The first term corresponds to the contribution of the solution compartment, which is similar in the heterogeneous and homogeneous systems. Additional quenching originates in the second term and increases for a larger $(1 - q)$ value, i.e., for a lower escape ratio. A plot of the β_{app} values obtained for different substrates in presence of Mo-LDH-**2** (Table 1) versus reported β values gives a straight line ($R^2 = 0.998$) in accordance to eq 8 (figure not shown). A volume fraction f of 1.7% and a k_{in} of $(3.6 \pm 0.4) \times 10^3$ s^{-1} can be calculated from the slope and from the intercept, respectively.

Notice also that the data of Table 1 prove that, at high Mo content, $^1O_2$ escapes even less efficiently from its locus of origin to the bulk of the solution. This drop in oxidant efficiency is easily explained taking into account the presence of intercalated molybdate for the molybdate-rich samples in addition to surface adsorbed molybdate. Singlet oxygen generated in the interior of the interlayers is obviously quenched very effectively.

To assess the surface quenching of singlet oxygen and its effect on the overall oxidant efficiency, LDH supports were doped with various amounts of Ni^{+2} (Mo-LDH-**9** to Mo-LDH-**12**; see Table SI1 in Supporting Information). Ni^{2+} with the characteristic absorption at 8500 cm^{-1} due to $^3A_g \rightarrow {}^3T_{2g}$ d$-$d electron transition[16] is known to deactivate $^1O_2$ in solution with a bimolecular rate constant comparable to the oxygenation rate of DMB by $^1O_2$ (viz. $k_q^{Ni} = 3.3 \times 10^7$ M^{-1}s^{-1}, whereas $k_r^{DMB} = 3 \times 10^7$ M^{-1}s^{-1}).[16] DMB peroxidation with the Ni-containing LDH-MoO$_4^{2-}$ hardly showed the formation of DMBO$_2$, despite the gradual consumption of H_2O_2 and the formation of the typical red-brown color of the tetraperoxomolybdate Mo(O$_2$)$_4^{2-}$. Since the concentration of soluble Ni^{2+} does not exceed the ppb level, deactivation by solubilized Ni^{2+} does not compete with the hydroperoxidation of DMB, i.e., [DMB]$k_r \gg$ [Ni^{2+}]k_q. Hence Ni^{2+} in the LDH structure is able to deactivate $^1O_2$. The observation that almost all $^1O_2$ is quenched on Ni-containing LDH thus supports the idea that $^1O_2$ molecules frequently collide with the LDH surface before they diffuse into the bulk solution where they react with DMB. As can be derived
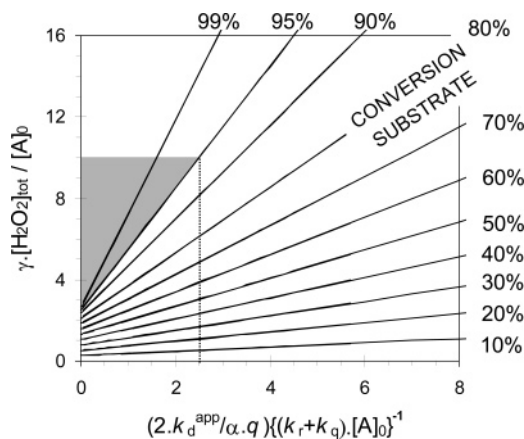
from Figure 8, $^1O_2$ is quenched more efficiently when more Ni is available in the LDH structure. Thus, successful peroxidation is governed by the efficiency of diffusion of $^1O_2$ through a deactivating zone between its origin at the surface and the bulk solution. In conclusion, deactivation results not only from quenching with ions and water molecules present in the polar double layer but also from frequent collisions with the LDH surface.

Simulation of the Peroxidation Reactions. A convenient way to study the peroxidation of organics with the LDH-MoO$_4^{2-}$/H$_2$O$_2$ system consists in transforming eqs 6 and 7 into 9, under the assumption that all H$_2$O$_2$ has been disproportionated ([H$_2$O$_2$]$_t$ = 0):

$$\frac{\gamma[H_2O_2]_{tot}}{[A]_0} = \left(\frac{2}{\alpha q}\right)X + \left(\frac{2}{\alpha q}\right)\left(\frac{k_{d,app}^A}{k_r + k_q}\right)\left(\frac{1}{[A]_0}\right)\ln\left\{\frac{1}{1 - X}\right\} \quad (9)$$

Here X is the conversion of the organic substrate A and $k_{d,app}^A = \beta_{app}(k_r^A + k_q^A)$. Values of β_{app} were reported in Table 1 for various substrates and catalysts. [H$_2$O$_2$]$_{tot}$ is the total concentration of oxidant that would be accumulated if the H$_2$O$_2$ had not been decomposed. Note that for a given catalyst/solvent system (e.g., Mo-LDH-**2** in MeOH), the value for $\alpha q = 2Y_{0,app}$ is directly obtained from Table 1. Finally, values for the rate constants of the substrate A, namely $k_r + k_q$, and for γ are known for many organic substances and were compiled in the review of Wilkinson.[16] The kinetic model can then be translated into a graphical form such as Figure 9, with different curves for different values of the substrate conversion X.

This graph allows estimating the required amount of oxidant to obtain a certain substrate conversion. As an example, the results of the peroxidation of 0.1 M DMB with 0.28 M H$_2$O$_2$ using Mo-LDH-**2** in MeOH can be simulated. Using Figure 9, the conversion of DMB at complete consumption of H$_2$O$_2$ is calculated at 88%, which is not so far from the 86% obtained experimentally (Figure 1).

A parity plot in Figure 10 illustrates the relatively small deviations between the observed data and the calculated data for many organic compounds. The experimental data were collected from experiments with various olefins such as presented in Table 2 and in ref 14b. Hence, the compartmentalization model enables a fair approximation of the experimental findings.

(20) (a) Iu, K.-K.; Thomas, J. K. *J. Photochem. Photobiol., A: Chem.* **1993**, *71*, 55. (b) Iu, K.-K.; Thomas, J. K. *J. Am. Chem. Soc.* **1990**, *112*, 3319. (c) Krasnansky, R.; Koike, K.; Thomas, J. K. *J. Phys. Chem.* **1990**, *94*, 4521. (d) Clennan, E. L.; Chen, M. F. *J. Org. Chem.* **1995**, *19*, 6004.
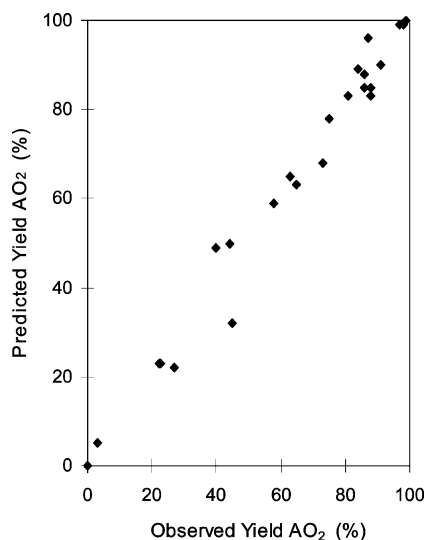
Figure 10. Parity plot for the kinetic model on Mo-LDH-**2**. Linear least-squares fit gives $R^2 = 0.988$. AO$_2$ = peroxide of substrate A.

The following general characteristics of $^1O_2$-mediated per-oxidations in the solid−liquid system can be extracted from the graph in Figure 9: (1) To maximize the oxidant efficiency, it is important to work with substrate concentrations as high as possible. (2) The oxidant efficiencies are higher for the more reactive substrates. (3) The maximum oxidant efficiency is determined by the type of catalyst used. The most efficient catalysts are those with the lower MoO$_4^{2-}$ loading. For instance, for Mo-LDH-**3**, the maximum efficiency for complete conversion can be estimated from Figure 9 by extrapolation to ∞ substrate concentration, giving a value of about 76%. Note that this value is considerably lower than the 92% obtained with the soluble MoO$_4^{2-}$.

Finally, it is important to note that the applicability of the Mo-LDH/H$_2$O$_2$ for synthetic peroxidations is restricted to sufficiently reactive organic compounds. This is easily derived from the graph. Suppose that the demanding requirements are at least 95% consumption of the starting material with at least 20% efficiency of the oxidant; it then follows that one has to work in the gray triangle in Figure 9. This means that $(k_r + k_q)[A]_0$ must be larger than 3.4×10^5, in case Mo-LDH-**3** is used as catalyst. Taking into account realistic substrate concentrations of 2 M, suitable substrates have rate constants k_r toward $^1O_2$ of at least 1.7×10^5 s^{-1} (and $k_q \sim 0$). The oxidation of less reactive substrates is practically not recommended with the LDH-Mo/H$_2$O$_2$ catalytic system, since these substrates require too much H$_2$O$_2$ to be fully converted.

Peroxidation of Unsaturated Organics on a Preparative Scale. In the batch reactions of Table 2, 1 g of Mo-LDH-**4** typically produces 1−10 g of the desired product, or 30−280 mol of product can be obtained/mol of exchanged MoO$_4^{2-}$. This highlights that the peroxidations are indeed catalytic in MoO$_4^{2-}$. As a comparison, the MoO$_4^{2-}$-exchanged resin of McGoran and Wyborney[13d] produces at most 0.5 mol of products/mol of Mo.

Besides the high productivity, the high activity of the Mo-LDH is also an appreciable advantage. For instance in the case of citronellol (**10**), 8.6 mol of product/mol of catalyst can be obtained/h, which is slightly higher than the activity (5.6 mol·(mol^{-1} h^{-1})) of the microemulsion catalytic system of Aubry et al.[22] Moreover, important advantages of the solid−

liquid system are the simple recovery of the solid Mo catalysts and the use of halogen-free solvents. One has to concede, however, that the use of the oxidant is somewhat less efficient due to competitive decay routes in the interior of the LDH granules.

Entries 1 and 2 focus on the nonradical bleaching of polyaromatic hydrocarbons in ambient conditions. Rubrene (**1**) and diphenylisobenzofuran (**2**) are frequently used as model substrates for such reactions. Both colored aromatics are cleanly converted into the colorless desired products.

Apart from these bleaching reactions, $^1O_2$ plays also an important role in the synthesis of some naturally occurring endoperoxides. Ascaridole (entry 3) was used as a remedy against mawworm and is the first endoperoxide which is produced by using $^1O_2$ on a preparative scale. Nowadays, if readily accessible, the endoperoxide is a promising reactive intermediate for the synthesis of monoterpene derivatives.[1] Ascaridole is also the pharmacologically active principle in a Peruvian medicinal plant, which has been used as nervine and antirheumatic drug.[22] The Mo-LDH/H$_2$O$_2$ is able to transform α-terpinene (**3**) almost completely into its 1,4-endoperoxide, ascaridole.

Singlet oxygen is also the oxidant of choice for the synthesis of allylic hydroperoxides. This route is even more promising than the classical autoxidation because of selectivity reasons. Entries 4−14 summarize the results for several cyclic and aliphatic olefins. Typically, the affinity for $^1O_2$ increases with the degree of alkyl substitution of the double bond (compare entries 4 with 5). Consequently, 2,3-dimethyl-2-butene (**3**) needs less H$_2$O$_2$ than 2-methyl-2-pentene (**4**) for complete reaction.

The typical regioselectivity of the $^1O_2$ hydroperoxidation is well preserved with the LDH-MoO$_4^{2-}$ catalyst. For instance, 1-methyl-1-cyclopentene (**6**) gives the three hydroperoxide products in the proper ratio of about 4:43:53. Regio- and stereoselectivity of the singlet oxygen reaction are demonstrated in entries 13 and 14. α-Pinene (**13**) forms only the *trans*-pinocarveyl hydroperoxide. The cis-compound is not formed due to steric hindrance of the bulky isopropylidene group toward attack of $^1O_2$. Note that by autoxidation at least three more hydroperoxides would be formed along with some carbonylic compounds.[1d] Likewise, only the *trans*-hydroperoxides of 2-carene (**14**) have been found. The product distribution, namely 24% endocyclic and 76% exocyclic allylic hydroperoxide, is essentially identical with those of photooxidized reaction mixtures.[23]

Reactions 8−12 and 15 are examples of industrial interest. The corresponding allylic alcohols of geraniol (**8**), nerol (**9**), citronellol (**10**), and linalool (**11**), which are easily obtained after reduction of the hydroperoxides, are useful precursors for substances in the fragrance chemistry (e.g., rose oxides from citronellol).[1] The hydroperoxide of terpinolene (**12**) is used for the manufacture of terpineol, whereas the hydroperoxide of mesitol (**15**) is a valuable intermediate in the synthetic route to vitamin E.[24]

(21) Lever A. B. P. *Inorganic Electronic Spectroscopy*; Elsevier: London, 1984.
(22) Okuyama, E.; Umeyama, K.; Saito, K.; Yamazaki, M.; Motoyoshi, S. *Chem. Pharm. Bull.* **1993**, *41*, 1309.
(23) Gollnick, K. *Adv. Photochem.* **1968**, *6*, 78.
(24) *Ullmann's Encyclopedia of Industrial Chemistry*, 6th ed.; Electronic Release, 1998.

It is important to notice that, in the latter case (entry 15), the use of Mo-LDH is not an attractive option due to the extremely low oxidant efficiency (about 4%). Nevertheless, on the basis of calculations with our kinetic model, mesitol belongs to the group of organic compounds that should be oxidized completely using at most 10 equiv of H_2O_2. This deviation can be rationalized if we take into account the basic properties of the LDH support. Indeed, due to this basicity, mesitol mainly exists in the suspension in its deprotonated form. Since it is known that the rate of physical quenching by phenolates is larger than their oxygenation rate, most of the $^1O_2$ is lost as $^3O_2$.[16]

Conclusion

The kinetics of oxygenation by singlet oxygen are well-known for homogeneous media but less for heterogeneous systems. For multiphasic media, the kinetics of $^1O_2$ reactions in microemulsions have been studied. The present work is the first detailed kinetic study of oxidation of organics by $^1O_2$, generated by a heterogeneous catalyst. As the solid catalyst, we have used the Mo-LDH material, which generates $^1O_2$ from H_2O_2. Especially for the production of hydroperoxides and endoperoxides derived from reactive substrates, i.e., with low Foote-index β values, this catalytic system is highly applicable. Although the yields based on H_2O_2 are somewhat lower in comparison with soluble molybdate, higher productivities are obtained as a result of the improved disproportionation rates.

A model has been elaborated that allows the estimation of the peroxide production in terms of reaction rates and oxidant efficiency. The model is based on Wilkinson's approach, and, in comparison with this approach, needs only two additional parameters in order to be practically useful for the heterogeneous case: The α value expresses the fraction of H_2O_2 that is converted to $^1O_2$. The q value expresses the fraction of $^1O_2$ that diffuses out of the LDH catalyst particle before being quenched.

The efficiency of singlet oxygen trapping in the Mo-LDH/H_2O_2 system seems to depend on the location of the MoO_4^{2-} in the LDH granule. To improve activity and oxidant efficiency, work is in progress to manipulate the density and the polarity of the LDH powder and the location of the molybdate within the catalyst, e.g., by competitive exchange procedures.

Supporting Information Available: Physicochemical data for the catalysts and a full mathematical derivation of the compartmentalization model. This material is available free of charge via the Internet at http://pubs.acs.org.

JA065849F